

Interactions between stable spiral waves with different frequencies in cardiac tissue

Fagen Xie, Zhilin Qu, James N. Weiss, and Alan Garfinkel

*Department of Medicine (Cardiology) and Department of Physiological Science,
University of California at Los Angeles School of Medicine, Los Angeles, California 90095*

(Received 22 July 1998)

Using simulations of inhomogeneous cardiac tissue, we investigated interactions between multiple stable spiral waves of different frequencies. We found that spiral waves with slower frequencies (longer periods) are swept away by the fastest spiral wave. For a system in which two spiral waves with different frequencies are initiated, the rate at which the slower spiral wave is terminated is proportional to the inverse of the frequency difference. This suggests that the conjectured state of multiple stable spiral waves with distinct frequencies cannot exist in cardiac tissue with homogeneous conduction properties. [S1063-651X(99)01702-X]

PACS number(s): 87.10.+e, 05.45.-a, 87.17.Aa

Reentrant excitation, in which a wave of excitation “re-enters” territory it has previously excited, is clinically the most important mechanism of cardiac arrhythmias. Reentrant spiral waves as a substrate of cardiac arrhythmias were first predicted in theoretical cardiac models [1–10], and have been observed experimentally in real cardiac tissue [11–13]. In cardiac fibrillation, electrical activity becomes complex and disordered. The precise nature of the activity underlying this disordered state is controversial. Winfree [14] suggested that fibrillation could be modeled as “several pinned rotors.” Studying a homogeneous excitable medium based on the FitzHugh-Nagumo model [15], Winfree found that the model was capable of producing stable spiral waves (a stable spiral wave is defined as a spiral wave with a circular tip trajectory and constant period throughout this paper) with two different frequencies for the same parameter values. However, when two spiral waves with different frequencies were induced in the same tissue, interactions between them always led to conversion of the slower spiral wave to the faster frequency. Lee [16] also found that a stable spiral wave and a focal excitation producing a target wave with a different frequency could not coexist. In a recent study of the complex Ginzburg-Landau equation in a weak inhomogeneous domain [17], a faster spiral wave was found to suppress slower ones. While these results suggest that this phenomenon may occur generically, it is not clear whether multiple stable spiral waves can coexist in cardiac tissue. Here we further study interactions between stable spiral waves with different frequencies in a two-dimensional inhomogeneous excitable medium, using a more physiologically realistic cardiac model.

Ignoring microscopic cell structure, the electrical impulse conduction in cardiac tissue can be described by the partial differential equation

$$\partial V / \partial t = -I_{\text{ion}} / C_m + D \nabla^2 V, \quad (1)$$

where V is the membrane voltage (mV), $C_m = 1 \text{ F cm}^{-2}$ is the membrane capacitance, $D = 1 \text{ cm}^2/\text{s}$ is the diffusion coefficient. $I_{\text{ion}} = I_{\text{Na}} + I_{\text{si}} + I_K + I_{K1} + I_{Kp} + I_b$ is the total cellular transmembrane ionic current density from the Luo-Rudy ventricular action potential model [18]. $I_{\text{Na}} = \bar{G}_{\text{Na}} m^3 h j (V - 54.4)$ is the fast inward Na^+ current; $I_{\text{si}} = \bar{G}_{\text{si}} d f (V - E_{\text{si}})$

is the slow inward Ca^{2+} current; $I_K = \bar{G}_K x \bar{x} (V - 77)$ is the time-dependent outward K^+ current; and I_{K1} , I_{Kp} , and I_b , which are solely functions of V , are the time-independent outward K^+ current, plateau K^+ current, and background current, respectively. m , h , j , d , f , and x are gating variables, all governed by the same type of linear ordinary differential equation. For details of the equations and functions see Ref. [18]. In our simulations we set $\bar{G}_{\text{Na}} = 23 \text{ mS/F}$, $\bar{G}_K = 0.282 \text{ mS/F}$, $\bar{G}_{\text{si}} = 0 \text{ mS/F}$, and $j \equiv 1$. These parameters yield a stable spiral wave in homogeneous tissue. We integrated Eq. (1) in a square sheet of tissue with no-flux boundary conditions: $\partial V / \partial x|_{x=0} = \partial V / \partial x|_{x=L} = \partial V / \partial y|_{y=0} = \partial V / \partial y|_{y=L} = 0$, where L is the tissue length. We used a well-known operator splitting method [19] with a variable time step (0.01–0.1 ms) to integrate the equations numerically, with a space step of 0.025 cm.

To reflect the electrophysiological heterogeneity of the real tissue, in which there is regional variation in cycle lengths, we modified the maximum conductance of the time-independent K^+ current I_{K1} , whose equation is $I_{K1} = \bar{G}_{k1} (V - V_{k1})$. \bar{G}_{k1} was modified to be a function of location within the tissue. In the original model, $\bar{G}_{k1} = 0.6047 \text{ mS/F}$. Here we choose $\bar{G}_{k1}(x, y)$ as

$$\bar{G}_{k1}(x, y) = \begin{cases} 0.6047 \text{ mS/F}, & x \leq L/2, y \leq L/2 \\ 0.5140 \text{ mS/F}, & x \leq L/2, y > L/2 \\ 0.4233 \text{ mS/F}, & x > L/2, y \leq L/2 \\ 0.3326 \text{ mS/F}, & x > L/2, y > L/2. \end{cases} \quad (2)$$

Thus the action potential duration of cells differs from region to region, since decreasing \bar{G}_{k1} prolongs the action potential duration. As a consequence, spiral waves in the four regions have different rotation periods or frequencies.

The interaction over time of four stable spiral waves initiated in the four regions (a – d) of the tissue ($7.5 \times 7.5 \text{ cm}^2$) is shown in Fig. 1(a). Initially, the four spiral waves coexist. Then the slowest spiral wave in the d region is progressively invaded by the other spiral waves with faster rotation frequencies. Eventually, the wave fronts of the other spiral waves collide with the tip of the slowest spiral wave, and drive it to the boundary, where it terminates. In a similar

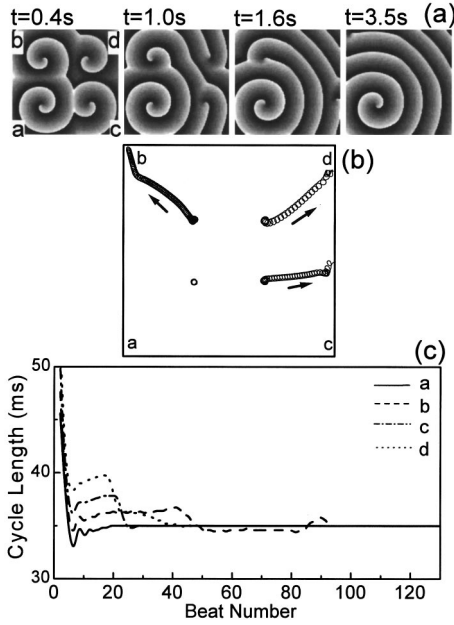


FIG. 1. Interactions between four stable spiral waves with different frequencies in electrophysiologically inhomogeneous tissue. (a) Snapshots at various times after initiation (at $t=0$) of the four spiral waves. White indicates depolarized tissue, and black repolarized tissue. (b) Trajectories of the tips of the four spiral waves over time. (c) The cycle lengths near the four corners ($a-d$) vs the beat number. The spiral waves with slow frequencies are gradually pushed to the boundary where they terminate. The system eventually selects the frequency of the fastest spiral wave.

fashion, the slowest of the remaining spiral waves is next pushed to the boundary and terminates, and this process is repeated until the system is finally dominated by the fastest spiral wave (with the shortest cycle length or period) and selects its unique frequency.

The motions of the tips of the four spiral waves are also shown in Fig. 1(b). As described above, the tips of all slower spiral waves drift to the boundary and disappear. The cycle lengths in each region (measured near the four corners) versus the beat number are shown in Fig. 1(c). The cycle length of each slower spiral wave is almost constant until the spiral wave disappears at the boundary, at which point that region assumes the shorter cycle length of the fastest spiral wave. The larger the cycle length difference with respect to the fastest spiral wave, the shorter the time to termination. Suppose the cycle lengths of two spiral waves are $T_1(f_1 = 1/T_1)$ and $T_2(f_2 = 1/T_2)$ ($T_1 < T_2$, $f_1 > f_2$). Then the drifting speed ν of the tip of the slower spiral wave is approximately proportional to its difference in frequency with the faster spiral wave [17,20]:

$$\nu \propto |f_1 - f_2|. \quad (3)$$

If the distance from the tip of the slower wave (f_2) to the boundary is D , then the disappearance time of the slower wave is approximately

$$T \approx \frac{D}{\nu} \propto \frac{D}{|f_1 - f_2|}. \quad (4)$$

If D is constant, then

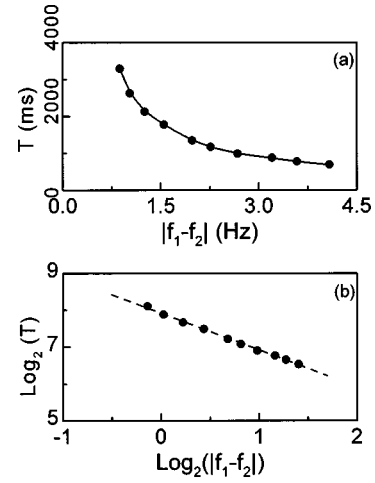


FIG. 2. Plot (a) and log-log plot (b) of the termination time (T) vs the frequency difference between two stable spiral waves. The dashed line in (b) is the theoretical line. The simulation data agree well with the theoretical line.

$$T \propto \frac{1}{|f_1 - f_2|}. \quad (5)$$

To test the above argument, we divided the tissue (here, the size is $5.0 \times 5.0 \text{ cm}^2$) into two equal parts from the center line $x=L/2$. We set $\bar{G}_{k1} = 0.6047 \text{ mS/uF}$ in the left region, and varied \bar{G}_{k1} in the other region. Therefore, the frequency of the spiral wave in the left region was constant, and the frequency of the spiral wave in the right region varied with \bar{G}_{k1} . In each simulation, we used identical initial conditions to initiate two spiral waves, so that the distance D in Eq. (4) for all initiated spiral waves is nearly constant. Figure 2 shows the relationship between the termination time T versus

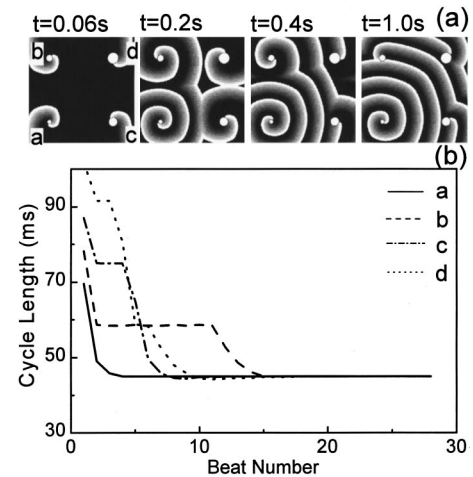


FIG. 3. Interactions between four anchored spiral waves with different frequencies in a tissue ($15 \times 15 \text{ cm}^2$) with four circular obstacles of different sizes. (a) Snapshots at various times after initiation (at $t=0$) of the four spiral waves. (b) The cycle lengths near the four corners ($a-d$) vs the beat number. Each anchored spiral wave with slow frequency rotates several times (the plateau) before it is entrained by the fastest spiral wave. The final state of the system is governed by the anchored spiral wave with the fastest frequency.

the frequency difference between the two spiral waves [Fig. 2(a), and their log-log plots [Fig. 2(b)]. As the difference between the two frequencies becomes small, the termination time T dramatically increases. The dashed line in Fig. 2(b) is the theoretical line according to Eq. (5), and shows close agreement with data from simulation (solid dots).

In the above analysis, the frequencies of the spiral waves were altered by changing the properties of the cellular action potential model (by varying \bar{G}_{k1}). It is also possible to alter spiral wave frequency by “anchoring” the spiral wave to defects of variable size, without changing the cellular action potential model. To extend our analysis to this situation, we created four circular obstacles with different sizes in a homogeneous tissue ($15 \times 15 \text{ cm}^2$). We then initiated four spiral waves anchored to the four obstacles which rotated with different frequencies (cycle lengths). The interaction over time between the four anchored spiral waves is shown in Fig. 3(a). Initially four anchored spiral waves each rotated around their obstacles several times, then the anchored spiral wave with the fastest frequency gradually invaded the whole tissue. Instead of disappearing completely, the slower anchored spiral waves continued to rotate around part of their obstacles, but could not complete a full rotation before the wave front from the fastest spiral wave arrived, causing them to become entrained to the fast spiral wave [15,16]. The system, therefore, selected the cycle length of the fastest spiral

wave. The cycle lengths near the four corners marked by $a-d$, respectively, versus the beat number, are shown in Fig. 3(b), and are similar to that of Fig. 1. *Again, the system goes to a final state with a unique frequency.* Since here the anchored spiral waves just need to become entrained to the fastest frequency rather than pushed to the boundary, the system arrived at the final state much sooner than in Fig. 1.

In conclusion, we have presented simulations demonstrating that for systems containing stable spiral waves (“functional” or anchored) with different frequencies, all spiral waves with slower frequencies are swept away by the fastest spiral wave, so that the system is always dominated by the fastest spiral wave. This may be the case even in generic excitable media, but it is especially important to cardiac tissue. Recently, in describing cardiac fibrillation Winfree [14] conjectured that “Several pinned rotors [anchored spiral waves in our terminology] would collectively resemble fibrillation.” Our results suggest this hypothesis is unlikely in a medium with homogeneous conduction properties. In such a medium, it is necessary for a spiral wave to at least become unstable (i.e., to enter a meandering or breakup regime) to resemble cardiac fibrillation [8–10].

This work was supported by NIH Grant No. P50 HL52319 and by the American Heart Association, greater Los Angeles affiliate (F.X. and Z.Q.).

-
- [1] A. Karma, Phys. Rev. Lett. **65**, 2824 (1990); **71**, 1103 (1997).
 - [2] A. Winfree, Chaos **1**, 303 (1991).
 - [3] D. Barkley, Phys. Rev. Lett. **68**, 2090 (1992).
 - [4] M. Bar and M. Eiswirth, Phys. Rev. E **48**, R1635 (1993).
 - [5] H. Zhang and A. Holden, Chaos Solitons, Fractals **5**, 661 (1995).
 - [6] D. Kessler *et al.*, Physica D **70**, 115 (1995).
 - [7] I. Efimov *et al.*, Chaos Solitons, Fractals **5**, 513 (1995).
 - [8] A. Karma, Chaos **4**, 461 (1994).
 - [9] M. Courtemanche, Chaos **6**, 579 (1996).
 - [10] A. V. Panfilov and P. Hogeweg, Science **270**, 1223 (1995).
 - [11] M. Allesie *et al.*, Circ. Res. **33**, 54 (1973); **39**, 168 (1976); **41**, 9 (1977).
 - [12] J. Lee *et al.*, Circ. Res. **78**, 660 (1996).
 - [13] J. Davidenko *et al.*, Nature (London) **355**, 349 (1992); A. Pertsov *et al.*, Circ. Res. **72**, 631 (1993).
 - [14] A. T. Winfree, Science **266**, 1003 (1994).
 - [15] A. Winfree, Physica D **49**, 125 (1991).
 - [16] K. J. Lee, Phys. Rev. Lett. **79**, 2907 (1997).
 - [17] M. Hendrey *et al.* (unpublished).
 - [18] C. Luo and Y. Rudy, Circ. Res. **68**, 1501 (1991).
 - [19] G. Strang, SIAM (Soc. Ind. Appl. Math.) J. Numer. Anal. **5**, 506 (1968).
 - [20] T. Bohr *et al.*, Physica D **106**, 95 (1997).